Computational Modeling of the Stability of Crevice Corrosion of Wetted SS316L

Fushuang Cui, Francisco J. Presuel-Moreno, Robert G. Kelly
University of Virginia, Department of Materials Science and Engineering
116 Engineer's Way, P.O. Box 400745, Charlottesville, VA 22903

ABSTRACT

The stability of localized corrosion sites on SS 316L exposed to atmospheric conditions was studied computationally. The localized corrosion system was decoupled computationally by considering the wetted cathode and the crevice anode separately and linking them via a constant potential boundary condition at the mouth of the crevice. The potential of interest for stability was the repassivation potential. The limitations on the ability of the cathode that are inherent due to the restricted geometry were assessed in terms of the dependence on physical and electrochemical parameters. Physical parameters studied include temperature, electrolyte layer thickness, solution conductivity, and the size of the cathode, as well as the crevice gap for the anode. The current demand of the crevice was determined considering a constant crevice solution composition that simulates the critical crevice solution as described in the literature. An analysis of variance showed that the solution conductivity (expressed as the chloride concentration) and the length of the cathode were the most important parameters in determining the total cathodic current capacity of the external surface. A semi-analytical equation was derived for the total current from a restricted geometry held at a constant potential at one end. The equation was able to reproduce all the model computation results both for the wetted external cathode and the crevice and give good explanation on the effects of physiochemical and kinetic parameters.

Keywords: Localized corrosion, modeling, stainless steel, atmospheric corrosion, repassivation potential

INTRODUCTION

Corrosion resistant materials such as stainless steels or nickel-based alloys may be subject to crevice corrosion initiation under atmospheric exposures at inherent geometrical crevices and other occluded geometries induced by oxide scales and precipitates which promote formation of aggressive chemistry. However, in order for such crevice corrosion to cast a structural integrity challenge, it must stabilize. Stability can only be maintained if the conditions within the occluded region remain sufficiently aggressive as to keep at least a portion of the crevice corroding actively. Not only must

the anodic kinetics within the crevice be sufficiently fast that the occluded solution remains a concentrated metal chloride solution despite diffusion and migration out of the crevice, but also the external cathode must be sufficiently robust in order to consume electrons generated by the anodic reactions. Obviously, ionic and electrical connectivity between anode and cathode must be maintained as well. [1-3]

Historically, crevice corrosion modeling has assumed a constant potential at the crevice mouth [4-6]. In some cases, the external cathode and the crevice have been modeled simultaneously in one code[7-9]. The former method sets a potentiostatic condition that is unrealistic in practice, due to the limitations in throwing power of a wetted (rather than immersed) surface [10]. The latter method makes separation of the effects of the crevice versus the external cathode more difficult. An alternative approach is to computationally separate the external cathode and the anode (the crevice) and then model them individually while the two are linked through a common fixed potential at the crevice mouth. Such a separation allows in-depth study of parameters characteristic to cathode and anode respectively. Indeed, using this approach, effects of physiochemical and kinetic parameters on the cathodic current limitation of wetted SS 316 at 25°C has been studied and meaningful insights of practical significance were obtained [10]. The reported repassivation potential of the crevice was used as it represents a critical point of stability.

As for the previous study [10], CREVICER, an object-oriented code, was extended to study the thin electrolyte system serving as the cathode as well as the anodic crevice. Unlike many published models which assume linear or simple Tafel electrochemical boundary conditions [11-13], this model uses polarization curves constructed based on experimental data. Detailed description of this model can be found elsewhere. [10]

In the present study, the effects of temperature on the limitation of wetted SS 316L to act as a cathode was studied. In addition, preliminary calculations on the demands of a crevice of SS 316L at 25°C are also reported. The total net cathodic current I_{net} that the cathode can support and the total anodic current I_{Lc} within the crevice were selected as output parameters of interest. The effects of kinetic and physiochemical parameters on I_{net} were studied while the effect of crevice gap size on I_{Lc} was explored as well. The projected I_{net} and I_{Lc} at 25°C were then compared to determine stability of the crevice. In addition, an attempt was also made to advance understanding on the observed effects of various parameters on I_{net}. A semi-analytical equation was consequently derived which projected identical I_{net} to computation results and rationalizes the observed effects of the parameters of interest.

MODEL DESCRIPTION AND BOUNDARY CONDITIONS

The model shown in Figure 1.a was used to simulate the atmospheric exposure of a SS 316L substrate covered by a layer of electrolyte thin film and containing a creviced region. The wetted surface (cathode) was assumed to have a varying length of Lc and the crevice (anode) was assumed to have a constant depth of 1 cm. It was assumed that both the wetted cathode surface and crevice had a constant width of 10 mm (an arbitrarily-picked value small enough to; the choice of this value has no effect on results). The

surfaces were, as illustrated in Figure 1.b, simulated with meshes generated by ANSYS®. The concentration of elements, as illustrated in Figure 1.b, was highest close to the crevice mouth where the potential/current density gradients were expected to be highest. The electrolyte thin film was assumed to be homogeneous (constant conductivity) and have a constant thickness of WL while the crevice was assumed to have a uniform gap size and a homogeneous solution (assumed to be the critical chemistry). As stated earlier, the cathode and anode were modeled separately .

The Cathode—The External Wetted SS 316L Surface

A full description of the FEM model used to study wetted SS316L surface at 25 ^{o}C has been presented elsewhere [10], and the present study used the same model to investigate the system at 95 ^{o}C. The increase of temperature brings changes in conductivity, oxygen solubility and diffusion coefficient, and kinetic parameters (E_{rp}, $E_{o,c}$, $i_{o,c}$, E_{corr}, β_c, and i_p). Realistic values of these parameters were chosen based on a literature search. [14-23] For example, the conductivity of the same solution at 95^{o}C was estimated to be 30% higher than at 25^{o}C [14], while O_2 diffusion coefficient was estimated to be $5.5 \cdot 10^{-5}$ cm^2/s at 95^{o}C (at room temperature, D=$1 \cdot 10^{-5}$ cm^2/s was used). [15]

The model outputted potential (E) and net cathodic current density ($i_{net}=i_c-i_p$) distribution profiles. A total net cathodic current I_{net}, the cathodic current that the thin-electrolyte cathode can use to support a localized corrosion site, was calculated by integrating the net cathodic current over all of the elements.

A full 3^3 factorial design of water layer (WL), chloride concentration ([Cl^-]) and length of cathode (L_c) was performed to explore the possible effects of these parameters as well as their possible interactions. Table 1 lists the parameter values used.

Table 1. Values of WL, [Cl^-] and L_c used in a full factorial design

WL (μm)	[Cl^-] (M)	L_c (cm)
10; 25 ; 200	0.001; 0.05; 1	0.25; 1 ; 10

For these calculations (base cases), the same kinetic parameters were used as shown in Table 2. Figure 2 shows the schematic of corresponding polarization curves: the oxygen reduction reaction (i_c, empty squares) in an electrolyte film with WL=10 μm and [Cl^-]=1 M; the passive behavior of the stainless steel (i_p, solid vertical line) and the summation of the two (i_c-i_p) (thick solid line, which overlaps with i_c at potentials well below E_{corr}). When the WL increases, the limiting current density decreases significantly due to the increase in the effective boundary layer thickness, as shown in Figure 2. However, as highlighted by the shaded zone, the SS 316L is expected to be under activation control in the range of potentials of interest of this study. Also shown in this figure is the i_c-i_p (filled triangles) of an electrolyte film with WL=10 μm and [Cl^-]=1 M at 25 ^{o}C. Raising temperature has a significant impact on kinetic behavior of SS 316.

Table 2. Values of kinetic parameters used in the base cases at 95°C

$E_{o,c}$ V	E_{rp} V	E_{cor} V	i_p A/cm^2	$i_{o,c}$ A/cm^2	i_{lim} A/cm^2	β_c V/dec
-0.05	-0.40	-0.15	10^{-7}	10^{-8}	$\frac{4FDC}{WL}$	0.1

The effects of each kinetic parameter (E_{rp}, i_p, $i_{o,c}$, and β_c) were studied by performing full factorial designs of Lc and [Cl^-] shown in Table 3. To save calculation time, however, only WL=25 μm was considered, and yet the number of calculations still amounted to 99 (=11 x 9). The effect of temperature was also discussed by comparing to results from a previous study. [10]

Table 3. Values of parameters used to exam their effects on total net cathodic current I_{net}

E_{rp} (V)	i_p (A/cm^2)	$i_{o,c}$ (A/cm^2)	β_c (V/dec)
-0.3, -0.4, -0.5	10^{-6}, 10^{-7}	10^{-7}, 10^{-8}, 10^{-9}	0.06, 0.1, 0.13

* For each parameter, full factorial design of L_c and [Cl^-] was used while WL was fixed at 25 μm

The Anode—The 316L Within The Crevice

In the present study the anode was modeled by a crevice with the crevice mouth held at the repasivation potential. Figure 3 show the electrochemical kinetics used, which were abstracted from that of Salamat et al. [24] who studied the kinetics of SS 316L in solutions designed to mimic the critical crevice composition. The anode (crevice) was L = 1 cm deep. Three gap (G) sizes were investigated (G=1, 10 and 25 μm), the solution had a conductivity (σ) equivalent to 5 M NaCl, and a pH of 0.75. The potential at the crevice mouth was E_{rp}= -0.35 V_{SCE} which was based on the literature.[17] Table 4 shows the values of kinetic parameters used in the base cases. The calculations did not consider chemical composition changes within the crevice. They thus represent a first-order estimate of the current demand of a crevice at the repassivation potential containing the assumed critical chemistry.

Table 4. Values of kinetic parameters used in computation of crevice current

E_{cor} V	E_{rp} V	$i_{o,a}$ A/cm^2	β_a V/dec	E_{aSS}	$i_{o,c}$ A/cm^2	β_c V/dec	E_{cHER}
-0.357	-0.35	10^{-6}	0.06	-0.825	10^{-8}	0.160	0.0975

The output of interest was the total current demand from the crevice which was obtained by integrating the calculated current density profile over the length of the crevice.

RESULTS

The Cathode—The External Wetted SS 316L Surface

Typical Current And Potential Distribution. Figure 4 shows typical potential and corresponding net cathodic current density distributions calculated from the model. As expected, the potential of cathode interface increased away from E_{rp} towards the E_{cor} of

the cathode with increasing distance from the crevice, while the corresponding net cathodic current i_{net} decreased simultaneously. Figure 4 also supports the selection of the graded meshing assuming that the potential/i_{net} gradients are the highest at elements adjacent to the crevice mouth. In addition, the figure indicates that the chloride concentration has a significant effect on the potential/current distributions.

Base Cases. A 3^3 full factorial design of water layer thickness (WL), length of cathode (L_c) and chloride concentration ($[Cl^-]$) was performed and Figure 5 shows the main effects of these parameters. Each data point in the figure corresponds to the summation of nine cases (the full factorial design of the other two parameters at three levels other than the fixed parameter). Evidently, all three parameters (WL, L_c and $[Cl^-]$) have significant impact on I_{net}; higher WL, L_c, or $[Cl^-]$, within the testing range, resulted in higher I_{net}.

A standard analysis of variance [25] was performed on the results from the full factorial design of WL, L_c and $[Cl^-]$, and the sum of squares was normalized with respect to the sum of square of WL. Table 5 lists results of the analysis, showing that WL, L_c, $[Cl^-]$, as well as the interactions of WL x L_c, and L_c x $[Cl^-]$ are of significance. The effects of interactions of WL x $[Cl^-]$ and WL x L_c x $[Cl^-]$ were very small. The interactions of WL x L_c and $[Cl^-]$ x L_c is indeed evident as shown in Figure 6. For example, when $[Cl^-]$ was 0.001 M, the effect of increasing L_c was negligible as I_{net} remained essentially constant; however, when $[Cl^-]$ was 1 M, I_{net} increased from 7.0×10^{-9} to 1.95×10^{-8} A when L_c increased from 0.25 cm to 10 cm. In addition, this figure also suggests that I_{net} saturates as L_c increases. This issue will be addressed in more detail in the Discussion section.

Table 5. Analysis of Variance for the full factorial design of WL, L_c, and $[Cl^-]$ at 95 ^oC

Source of Variance	WL	L_c	$[Cl^-]$	WLx L_c	WLx$[Cl^-]$	L_c x$[Cl^-]$	WLx L_c x$[Cl^-]$
Ratio to WL	1	1.97	4.74	0.60	0.24	1.28	0.36

Based on the magnitude of normalized sum square listed in Table 5, the effects of these five parameters follows the ranking: $[Cl^-] > L_c > L_c$ x $[Cl^-] >$WL> WL x L_c. The effect of WL is rather small and this is likely because the SS 316L is under activation control in the range of potentials of interest and change in WL consequently has little effect on the corresponding cathodic reaction rate.

Effect of Temperature. The ratio $R_T = I_{net}(T=95^oC)/I_{net}(T=25^oC)$ was used to quantify the effect of temperature on I_{net}. As shown in Figure 7, by increasing temperature from 25 to 95^{o}C, I_{net} increased by a factor between 6 and 30. The figure also suggests that $[Cl^-]$, WL and Lc all have some interaction with temperature. For example, for a case with 1 M $[Cl^-]$ and a cathode of 1cm length, the R_T was as high as 21, whereas this R_T decreased to 6.5 for the same cathode with 0.001 M $[Cl^-]$. Despite the large variation of R_T with $[Cl^-]$ as well as WL at smaller L_c, it nevertheless reached a largely constant value (~6.50) as L_c increased to 10 cm (a value large enough so that I_{net} saturated).

Effects of Kinetic Parameters ($i_{o,c}$, E_{rp}, β_c, i_p). To quantify the effects of kinetic parameters ($i_{o,c}$, E_{rp}, β_c, and i_p) on total net cathodic current I_{net}, the following ratios were defined:

$R_c = I_{net}(i_{o,c}=10^{-7} \text{ or } 10^{-8})/I_{net}(i_{o,c}=10^{-9})$,
$R_{Erp} = I_{net}(E_{rp}=-0.4 \text{ or } -0.5)/I_{net}(E_{rp}=-0.3)$,
$R_{\beta c} = I_{net}(\beta_c=0.13 \text{ or } 0.1)/I_{net}(\beta_c=0.06)$, and
$R_a = I_{net}(i_p=10^{-6})/I_{net}(i_p=10^{-7})$,

where the units for the parameters are A/cm^2 for $i_{o,c}$ and i_p, V (vs SCE) for E_{rp}, and V/dec for β_c respectively. In general, a ratio that significantly deviates from 1 (>>1 for R_c and R_{Erp} and or <<1 for $R_{\beta c}$ and R_a) suggests a considerable effect of the corresponding parameter.

As shown in Figures 8-10, $i_{o,c}$, E_{rp} and β_c all have significant impact on I_{net} as values of R_c and R_{Erp} are significantly larger than 1 and values of $R_{\beta c}$ are always smaller than 0.2. For example, as shown in Figure 8, increasing $i_{o,c}$ by a factor of 10 resulted in an increase of I_{net} by a R_c between 4 and 11. In addition, these three figures also consistently suggest that L_c and [Cl^-] have significant impacts on the effect of these kinetic parameters ($i_{o,c}$, E_{rp} and β_c) respectively. Despite the large variation with [Cl^-] at smaller Lc, however, the ratios (R_c, R_{Erp}, and $R_{\beta c}$) tended to reach constant values as L_c increased. For example, as shown in Figure 9.a, R_{Erp} was 9.35, 7.05 and 3.59 for [Cl^-]=1, 0.05 and 0.001 M respectively. These values gradually decreased with increasing L_c and eventually reached one constant value (3.45) at L_c =10 cm.

The passive current density i_p was found to have a rather small impact on I_{net} in the tested range. Figure 11 shows that the change of i_p by a factor of 10 (from 10^{-7} to 10^{-6} A/cm^2) only results in a small change (~5%, R_a~0.95) in I_{net} though R_a varies slightly with choice of L_c and [Cl^-]. Similar to other kinetic parameter cases, R_a also reached a constant value (0.94) when I_{net} reached saturation at large L_c (10cm).

The Anode-The 316L within the Crevice

Typical Current and Potential Distributions. The potential and current distribution results from the computational modeling are shown in Figure 12. As expected, the potential falls monotonically with increasing distance into the crevice. High current densities are observed over up to 1 mm in from the mouth with the current density decreasing deeper into the crevice. The rate of decay of the current density depended strongly on the crevice gap, with larger gaps exhibiting higher currents deeper into the crevice.

Effect of Gap. Nobler potentials are observed deeper for the higher gap cases in Figure 12, *i.e.*, as the gap decreases, the potential profile becomes steeper over initial distances into the crevice, and then flattens out at deeper distances. In all three cases the potential at the tip (farthest in) of the crevice was at or very close to the OCP, hence the small currents at the corresponding depths. Figure 13 shows the total current demand of the crevice, I_{Lc}, as a function of gap, along with the results of power law fits to the results. The power law fits the data very well, with the exponent of 0.48.

DISCUSSION

Effects of Parameters on the Current from a Wetted Cathode

For a wetted cathode coupled to a localized corrosion site, the current and potential distribution along it as well as the total net cathodic current I_{net} are affected by many physicochemical and kinetic parameters such as water layer thickness (WL), size of cathode (L_c), [Cl^-], temperature (T), anodic and cathodic behavior of the cathode (i_p, $i_{o,c}$, β_c), and repassivation potential (E_{rp}). In a previous study on a wetted SS 316 cathode exposed at room temperature 25°C [10], the effects of WL, L_c and [Cl^-] was studied using a full factorial design using I_{net} as the characteristic of interest. The effects of kinetic parameters were also explored by parameterizing each parameter while holding the rest at base values. In this study, the same approach was used to characterize the effects of these parameters as well as increased temperature (95°C).

The effects of temperature on I_{net} were found to depend on the values of L_c, [Cl^-], and WL. The ratio of net currents for a given cathode case ranged from 6 to 30 depending upon the values of the physical parameters. The larger ratios occurred at smaller cathode lengths, and as the cathode reached a length that led to the saturation of I_{net} (cf. Figure 6), the increase in I_{net} upon an increase in temperature from 25°C to 95°C became approximately 6.5, independent of the values of the other parameters. Additional effects of temperature would be through effects on oxygen solubility, oxygen diffusion coefficient, and the kinetic parameters. The manifestation of these effects on the total current capability of the cathode is convoluted due to the interactions among them as indicated by the dependence of the various ratios shown in Figures 6-11.

The relative importance of the physical parameters, L_c, [Cl^-], and WL, and their interactions is similar to that found at 25°C [10], although at 95°C, the [Cl^-] is the most important parameter rather than the L_c. As at 25°C, the WL is of less importance in determining the current capacity of the cathode.

As observed at 25°C, simple linear regression of the results does not lead to acceptable abstraction. Linear regression using the five factors of significance identified by the analysis of variance results in the following expression:

$$I_{net} = 2.85\cdot10^{-12}\cdot WL + 6.74\cdot10^{-9}\cdot[Cl^-] - 7.32\cdot10^{-10}\cdot Lc + 1.10\cdot10^{-11}\cdot WL\cdot Lc + 2.94\cdot10^{-9}\cdot[Cl^-]\cdot Lc + 3.35\cdot10^{-9} \qquad R^2=0.80 \qquad (11)$$

The correlation coefficient is similar to that found using a similar approach at 25°C using five factors. The relatively poor performance of the linear regression can be attributed to the lack of inclusion of the effects and interactions with the kinetic parameters as well as the restriction to linear terms.

Semi-Analytical Expression of Current Capacity from a Restricted Geometry

In addition to the computational characterization, we have attempted to abstract our results into an equation that incorporates all the parameters of interest and rationalizes the modeling experimental observations. The approach has been to consider the restricted geometry of the wetted cathode and to introduce the concept of an equivalent cathode length, L_c, to account for the distribution of current along the cathode, as well as the introduction of the kinetics via a determination of an equivalent, or average, current density.

For a cathode with the same geometry considered in this study (Figure 1), assume

$$I_{net} = i_{eq} \cdot L_{eq} \cdot W \qquad \textbf{(assumption 1)} \tag{4}$$

where L_{eq} is the equivalent length of the cathode, W is the actual width of the cathode, i_{eq} is the equivalent current density, and I_{net} is the total net cathodic current

$$i_{eq} = \frac{\int_{E_L}^{Erp} (i_c - i_p) \cdot dE}{E_L - E_{rp}} = \frac{\int_{E_L}^{Erp} (i_c - i_p) \cdot dE}{\Delta E} \tag{5}$$

where E_L is the potential of the cathode edge which has the largest distance to the crevice mouth. It is apparent that if the cathode has a constant net cathodic current density along it length, then $L_{eq}=L_c$ and $i_{eq}=i_{lim}-i_p$

Assume that the electrolyte on the cathode surface acts as an ideal resistor with resistance R,

$$R = \frac{L_{eq}}{C \cdot \sigma \cdot WL \cdot W} \qquad \textbf{(assumption 2)} \tag{6}$$

so that the potential drop across the cathode can be estimated by

$$\Delta E = E_x - E_{rp} = I_{net} \cdot R = \frac{I_{net} \cdot L_{eq}}{C \cdot \sigma \cdot WL \cdot W} \qquad \textbf{(assumption 3)} \tag{7}$$

where σ is the conductivity of the electrolyte (assumed to be constant throughout the restricted geometry), and C is a geometric correction factor. This correction is needed as the electrolyte layer this is by no means a simple resistor which would have $R = \frac{Lc}{\sigma \cdot WL \cdot W}$. In the case of the wetted cathode, the electrolyte layer acts as a leaky resistor due to the interfacial current along its length.

Solve 7 for L_{eq} and substitute the result into equation 4

$$I_{net} = W \cdot \sqrt{C \cdot \Delta E \cdot \sigma \cdot WL \cdot i_{eq}} \tag{8}$$

and replace i_{eq} with equation 5

$$I_{net} = W \cdot \sqrt{C \cdot \sigma \cdot WL \cdot \int_{E_L}^{E_{rp}} (i_c - i_p) \cdot dE} \qquad (9)$$

Definition and Validation of a Value for C. The constant *C* characterizes the effects of the interfacial reactions on the effective resistance. To determine its value, the entire set of results was considered. When the square of I_{net} is plotted *versus* the product of *W*, *WL*, σ, and the integral, an excellent linear relationship was observed. The slope of the line was 2.0, with a correlation coefficient of 1.0. Thus,

$$I_{net} = W \cdot \sqrt{2 \cdot \sigma \cdot WL \cdot \int_{E_L}^{E_{rp}} (i_c - i_p) \cdot dE} \qquad (10)$$

In addition, equation 10 also successfully reproduced the observed effects (all R values shown in Figures 7-11) of temperature (changing temperature will result in change of σ and kinetic parameters) and all the kinetic parameters including $i_{o,c}$, E_{rp}, b_c and i_p. Table 6 lists the projections from equation 10 compared to the model outputs for selected cases with different temperature and kinetic parameters. In all cases, equation 10 yielded near identical results (error less than 0.4%) to the full model computation for the individual cases.

Table 6 Comparison of I_{net} projected by Equation 9 and the model computation for selected cases with various kinetic parameters or temperatures.

	95°C					25°C
	Base case	$i_{oc}=10^{-9}$ A/cm^2	E_{rp}=-0.3 V vs SCE	β_c=0.06 V/dec	$i_p=10^{-7}$ A/cm^2	Base case [10]
I_{net} (A/cm^2) projected by Equation 9	$7.312 \cdot 10^{-9}$	$2.196 \cdot 10^{-9}$	$2.197 \cdot 10^{-9}$	$3.785 \cdot 10^{-9}$	$6.836 \cdot 10^{-9}$	$1.131 \cdot 10^{-9}$
I_{net} (A/cm^2) projected by Model Computation	$7.314 \cdot 10^{-9}$	$2.188 \cdot 10^{-9}$	$2.190 \cdot 10^{-9}$	$3.790 \cdot 10^{-9}$	$6.839 \cdot 10^{-9}$	$1.129 \cdot 10^{-9}$
Error %	0.03%	0.36%	0.32%	0.13%	0.04%	0.18%

* All cases have 0.05M Cl^-, Lc=10cm, WL=25μm

For the use of equation 10, one challenge is the determination of E_L, the potential of the cathode edge furthest from the crevice mouth (*i.e.*, at L_c). In general, E_L increases with increasing L_c until the open circuit potential of the cathode, $E_{oc,}$ is reached. In this way, the effect of L_c is thus implicitly considered by this equation. Though in most cases estimation of E_L is not straightforward (in this study, values of E_L were determined from potential profiles outputted by the model calculations), its value is limited in that it can never exceed the open circuit potential of the cathode E_{oc}. Thus, equation 10 can be used to estimate the current limitation of cathodes by using E_{oc} for E_L.

Whereas equation 10 was derived in the context of the current capacity of the external, wetted cathode, it can also be directly applied to the case of a crevice, if the same conditions are operable. In the calculations presented here, these conditions (*i.e.*, constant conductivity, constant geometry, constant potential at the crevice mouth) are

operable. In the case of the crevice, the *WL* in equation 10 would be replaced by the gap, *G*, and the current being calculated would be that demanded by the crevice, I_{Lc}. Thus, one would obtain the following:

$$I_{Lc} = W \cdot \sqrt{2 \cdot \sigma \cdot G \cdot \int_{E_L}^{E_{rp}} (i_c - i_p) \cdot dE} \qquad (11)$$

Equation 11 represents a power law with respect to the gap G, all else being equal. Thus, it would predict that a plot of log I_{Lc} versus log G would result in a straight line with a slope of ½. Figure 13 shows such a plot for the data generated, and an excellent straight line is observed with a slope very close to ½.

These two abstractions can serve as the foundation for the estimation of crevice corrosion stability under atmospheric exposure conditions. For a given set of values of the physical parameters and electrochemical kinetics, the current capacity of the cathode, I_{net}, can be compared to the current demand from the crevice, I_{Lc}. If the former is equal to or exceeds the latter, the crevice can be stabilized by that cathode.

While the calculations for both the cathode and anode assume steady state conditions and uniform conductivity, they do represent a reasonable approach to abstracting the key parameters into a form that allows a first-order estimate of crevice stability. With time, the chemical conditions at the cathode will change and likely decrease the current capacity. Similarly, as the chemical conditions inside the crevice evolve, it is likely that the current demand will decrease, although as the crevice corrodes, the increase in surface area could lead to increased current demand.

Saturation of Cathodic Current I_{net}

Figure 6 shows that I_{net} saturates (reach a maximum value, called I_{max} hereafter) when L_c exceeds a critical value. This phenomenon was observed at 25°C as well [10] and it is obvious from equation 10 which allows quick calculation of I_{max} without going through resource-demanding modeling computation. The origin of this saturation can be ascribed to the fact that i_{net} (i_c-i_p) diminishes with distance to the crevice and eventually become zero when the open circuit potential of cathode is reached at a critical distance.

Figure 6 also shows that the I_{max} and corresponding L_c at which I_{max} is observed significantly increases with [Cl^-]. For example, I_{max} was reached when L_c was as small as 1 cm for a case with 0.001 M Cl^-, whereas I_{max} was only reached when L_c was 15 cm for a case with 1 M Cl^-. This is due to the increase of conductivity. Computations on cases with fixed WL=10 or 200 μm as well as fixed 0.001 or 1 M Cl^- were also performed and a similar saturation behavior of I_{net} was observed.

Table 7 Projected saturation limit for I_{net} at 95 °C

WL μm	10			25			200		
$[Cl^-]$ M	0.001	0.05	1	0.001	0.05	1	0.001	0.05	1
L_c (cm) needed for 98% I_{max}	0.25	1	4	0.25	4	10	1	10	15
98% I_{max} **(10^{-8}A)**	**0.066**	**0.46**	**1.92**	**0.102**	**0.73**	**3.04**	**0.265**	**1.87**	**7.5**

* Choice of kinetic parameters is listed in Table 2.

As discussed above and in an earlier report [10], the determination of I_{max} and the smallest cathode size at which I_{max} is realized are of practical importance, offering significant information to answer two important questions to atmospheric systems which often have patches of electrolytes rather than contiguous thin electrolyte films: (a) what size patch of electrolyte could support a sustained localized corrosion site; (b) how fast such a site could corrode. Because I_{max} is approached asymptotically, 98% I_{max} was used to determine required minimum Lc for current saturation and the results are summarized in Table 7. This type of table allows the determination of a practice maximum size of cathode. Further increase of cathode will not provide significant extra cathodic current (<2%). Such a table can also be used to determine stability of a localized corrosion site by coupling with the Galvele criterion [26] or using the approached discussed in next section.

Stability of Localized Corrosion

For systems under natural conditions, the stability of localized corrosion requires a cathode which can supply a cathodic current (I_{net}) that matches or exceeds the anodic current within the crevice (I_{Lc}). The anodic current demand is determined by the need to maintain a solution with a sufficiently aggressive composition that repassivation is prevented. Experimentally, this condition can be measured by determination of the repassivation potential of the crevice. Sridhar and colleagues [17,27,28] have shown that when properly determined, E_{rp} can be used as a criterion for crevice stability. However, determination of E_{rp} is done under conditions of full immersion and potentiostatic control. In natural systems, the role of the potentiostat is replaced by the external cathode. For conditions of full immersion in highly conductive solutions, increasing the cathode size linearly increases the current the cathode can supply.

For localized corrosion systems under atmospheric conditions, the restricted geometry of a wetted cathode limits the ability of the external cathode to provide current to the crevice at and above the repassivation potential. This limitation leads to an inherently increased instability for localized corrosion in atmospheric exposure. The work presented here provides a means to quantitatively assess the level of that instability. By determining I_{max} and comparing it to I_{Lc}, the stability of coupled localized corrosion site can be assessed. An application of this approach is showcased below considering a localized corrosion of SS 316L under atmospheric exposure at 25 °C.

Figure 13 represents the current demand from a 1-cm long crevice as a function of gap, assuming that the mouth is at the repassivation potential. The dotted horizontal lines

represent the maximum currents available from an external wetted cathode (I_{max}) assuming different WL values, but having the same solution composition (1 M NaCl). Thus, if the WL was 200 microns thick, a crevice with a gap of 2.3 microns could be supported, and decreasing the WL to 25 microns decreases the maximum gap that can be stabilized to 0.4 microns. Further decreasing the WL to 10 microns leads to a reduction in the maximum gap to 0.14 microns. The value for a 200 micron WL seems reasonable when compared to the 4 microns predicted by Lee and Kain [29] using the model of Oldfield and Sutton [30] for the critical gap for full immersion in seawater.

Such abstractions have utility not only in the design of experiments relevant to localized corrosion under atmospheric conditions, but also in the prediction of cathode/anode combinations that should be avoided to assure long-term integrity of a structure.

CONCLUSIONS

Crevice corrosion of SS 316L under atmospheric condition was studied by computational study of the external cathode and crevice separately. Effects of physiochemical and kinetic parameters on the total net cathodic current I_{net} and the effect of crevice gap size on the total anodic current I_{Lc} were explored. The I_{net} and I_{Lc} were used to determine stability of crevice corrosion. The following conclusions can be drawn:

For the cathode:

1. WL, Lc and [Cl^-], as well as the interactions of Lc and WL, and Lc and [Cl^-] have significant impact on the total net cathodic current I_{net}. An analysis of variance showed that the effects of these factors decrease in the following order: [Cl^-] > Lc>Lc x [Cl^-] >WL> WL x Lc.
2. Temperature (95 vs 25 ^oC) was found to have a significant effect on I_{net} with the increase in I_{net} ranging from a factor of 6 to a factor of 30, the value of which was dependent on the values of the other physical parameters. At large cathode sizes, L_c, the effect of temperature became independent of the other parameters and approached a value of 6.5.
3. Cathodic kinetic parameters, E_{rp}, $i_{o,c}$, and β_c, were found to have significant effects on I_{net}, whereas i_p in the cases of studied had little effect on I_{net}.
4. A semi-analytical equation was derived for the total current from a restricted geometry held at a constant potential at one end. The equation was able to reproduce all the model computation results both for the wetted external cathode and the crevice and give good explanation on the effects of physiochemical and kinetic parameters.
5. The total net cathodic current I_{net} was found to reach limiting values (I_{max}) as the cathode size L_c increased. The 98% I_{max} (used instead of I_{max} because I_{net} typically gets saturated very slowly) as well as the corresponding characteristic Lc of cases with various WL and [Cl^-] (each three 3 levels) were determined.

For the anode (25°C)

1. The total anodic current I_{Lc} was calculated for crevice assuming constant crevice chemistry.
2. In accord with the semi-analytical expression described above, I_{Lc} was found to increase in proportion to the square root of the crevice gap.

For the conditions considered in this study, the concept of localized corrosion stability projects that crevices at 25 °C can stabilize only if the crevice gap is smaller than 5 μm, with the exact value depending upon the physical parameters of the cathode.

ACKNOWLEDGEMENTS

This work was supported by the Office of Science and Technology International of the United States Department of Energy (DOE) and carried out as part of the DOE Multi-University Corrosion Cooperative under Cooperative Agreement DE-FC28-04RW12252. The funding agency is gratefully acknowledged.

REFERENCES

1. M.G. Fontana, Corrosion Engineering, 3rd Edition, 1986: p.53
2. H.W. Pickering, Corrosion 42, 3(1986): p. 125
3. R.K. Dayal, "Crevice Corrosion of Stainless Steel," in Corrosion of Austenitic Stainless Steel, Ed. By H.S. Khatak and B. Raj, 2002: p. 106
4. Y. Xu, H.W. Pickering, *J. Electrochem. Soc.*140, 3(1993): p. 658
5. J. S. Lee, M. L. Reed, R. G. Kelly, *J. Electrochem. Soc* 151, 7(2004): B423-B433
6. K.C. Stewart, Ph.D. Dissertation, Department of Materials Science and Engineering, University of Virginia, Charlottesville, VA (1999)
7. J.W. Oldfield and W.H. Sutton, British Corrosion Journal 15, 1(1980): p. 31
8. P.O. Gartland, in Proceedings of Corrosion/96 Research Topical Symposia, 311, NACE International, Houston, TX (1996)
9. R.W. Evitts, M.K. Watson and J. Postlethwaite, "Numerical Simulation of Crevice Corrosion of Titanium: Effect of Bold Surface" Corrosion96, 1996:P.121/1-121/10
10. F. Cui, F. J. Preseul-Moreno, R. G. Kelly, *Corrosion Science*, accepted May, 2005. (invited).
11. E. McCafferty, J. Electrochem. Soc. 124 (1977) 1896
12. P. Doig, P.E.J. Flewitt, Philosophical Magazine B, 38 (1978) 27
13. R. Morris, W. Smyrl, J. Electrochem. Soc. 135 (1988) 723
14. Y Zheng and J A Robers, J. Phys: Condens. Matter 8 (1996): p.8089
15. B. Case, Electrochmica Acta 18, 1973: p. 293
16. Kazuya Ohkubo, Kenkyusho Kenkyu Hokoku, 3 (2001): p. 2
17. D.S. Dunn, G.A. Cragnolino, N. Sridhar, Corrosion 56, 1(2000): p. 90
18. G.A. Cragnolino, D.S. Dunn, N. Sridhar, "Environmental Effects on Stress Corrosion Cracking of Type 316L Stainless Steel and Alloy 825 as High-Level Nuclear Waste Container Materials, CNWRA 94-028, 1994

19. Radoslav Adzic, “Recent Advances in the Kinetics of Oxygen Reduction”, in Electrocatalysis, Edited by Jacek Lipkowski and Philip N. Ross, Wiley-VCH 1998: p. 236
20. S.J. Clouser, J.C. Huang, E. Yeager, Journal of Applied Electrochemistry, 13(1993): p. 597
21. R. Biswas, S.N. Lvov, Z. Ahmad, Digby D. Macdonald, “Electrode-Kinetic And Corrosion Measurements in High Temperature Aqueous Environments”, in proceedings of the symposium on Electrode Materials and Processes For Energy Conversion and Storage IV, edited by J. McBreen, S. Mukerjee, S. Srinivasan, 1997: p. 340
22. Private communicate with N. Sridhar at South West Research Institute, 2005
23. N. Scridhar and G.A. Cragnolino, Corrosion 49, 11 (1993): p. 885
24. G. Samalat, G.A. Juhl, and R.G. Kelly, Corrosion 51,11,p832 1995
25. D.C. Montgomery, Design and Analysis of Experiments, 4th Edition, John Wiley & Sons, Inc. New York, NY 1997, p.441
26. J.R. Galvele, J. Electrochem. Soc., 123 (1976): p. 464
27. N. Sridhar, C.S. Brossia, D.S. Dunn, A. Anderko, Corrosion 60, 10(2004): p. 915
28. A. Anderko, N. Sridhar, D.S. Dunn, Corrosion Science 46, (2004): p. 1583
29. T. S. Lee, R. M. Kain, Paper 69, Corrosion/83, NACE, Houston (1983).
30. J. W. Oldfield, W. H. Sutton, British Corrosion Journal 13, (1978): p. 104

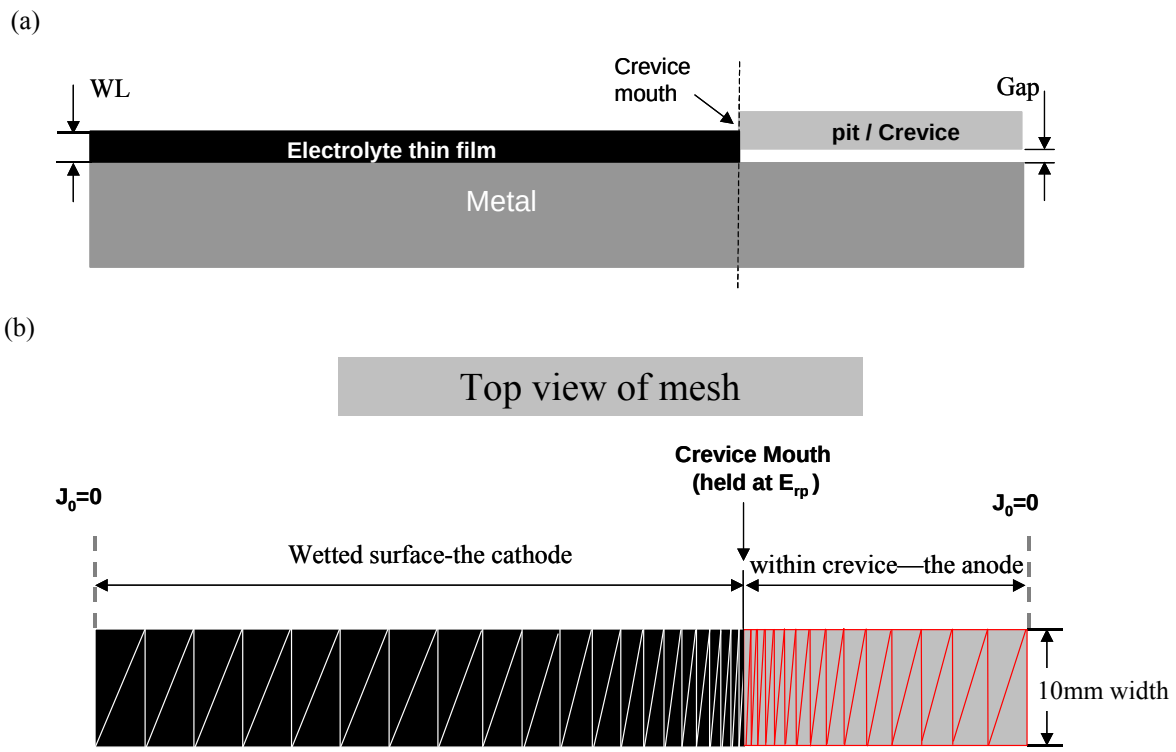

Figure 1. Schematic of the system modeled: a) a typical crevice corrosion system for atmospheric exposure; b) Top view of the mesh. The cathode and anode was separated and modeled individually. The two were linked by hold a common fixed potential E_{rp} (repassivation potential) at the junction point (crevice mouth).

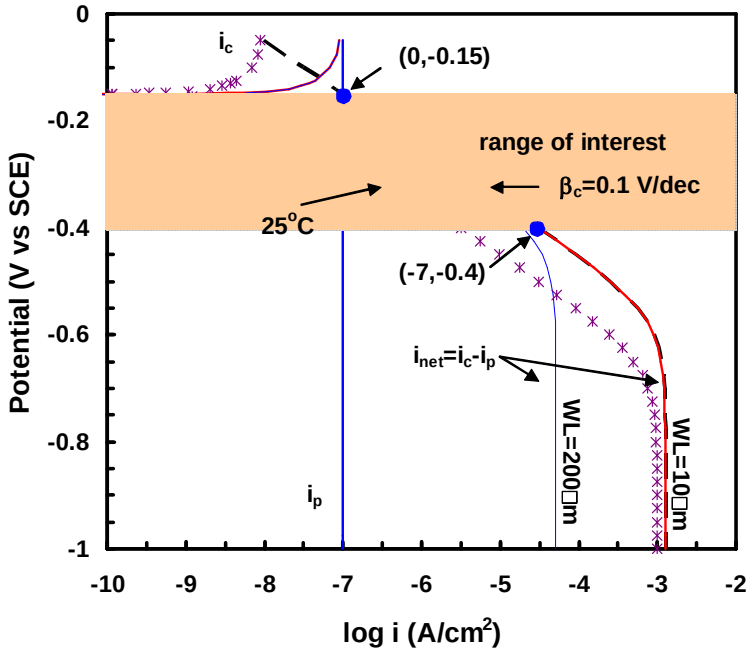

Figure 2. Cathodic and Anodic polarization curves used in base cases at 95°C

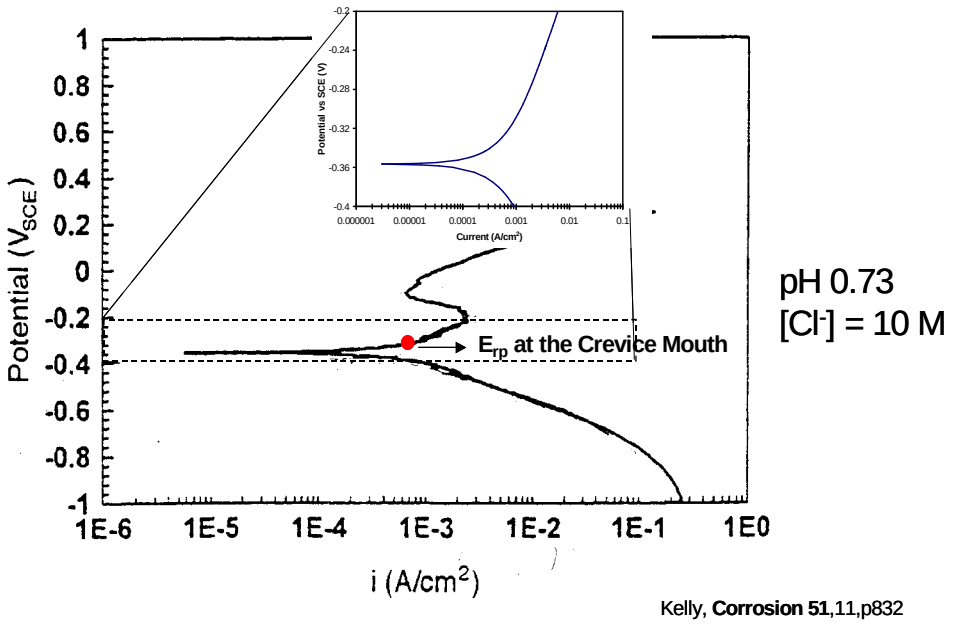

Figure 3. Electrochemical Kinetics for 316L in Critical Crevice Solution

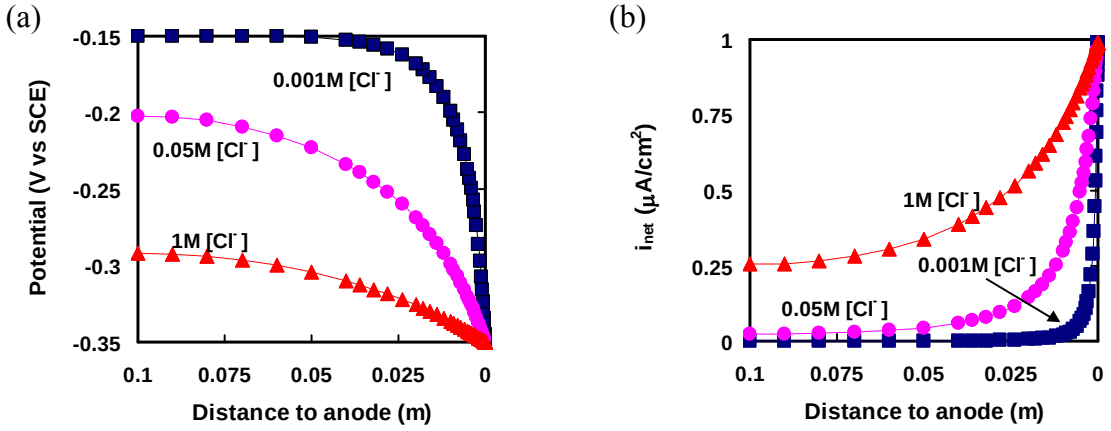

Figure 4. Typical Model Outputs for the cathode. Potential increased and i_{net} decreased with distance to anode. Elements near to the anode had the highest Potential/i_{net}, and [Cl$^-$] apparently had significant impact on the potential/current density distribution. (Base cases, WL=25 μm, Lc=10cm)

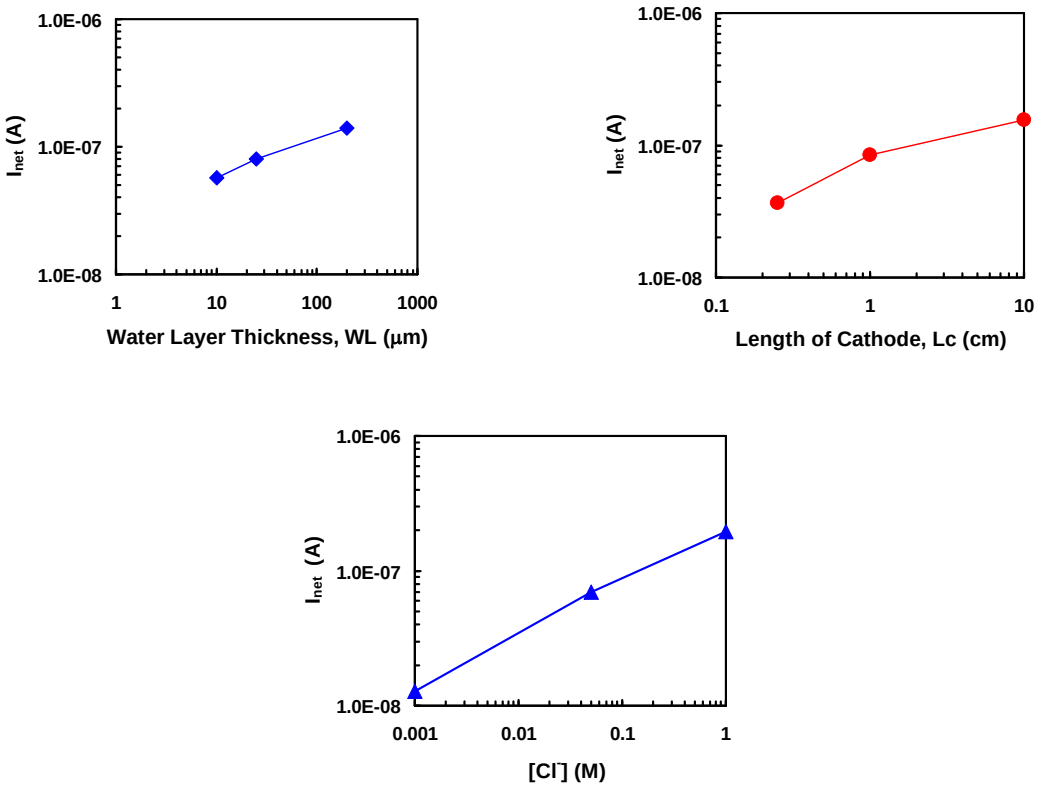

Figure 5. Main effect (95°C) of WL, Lc and Cl^-.

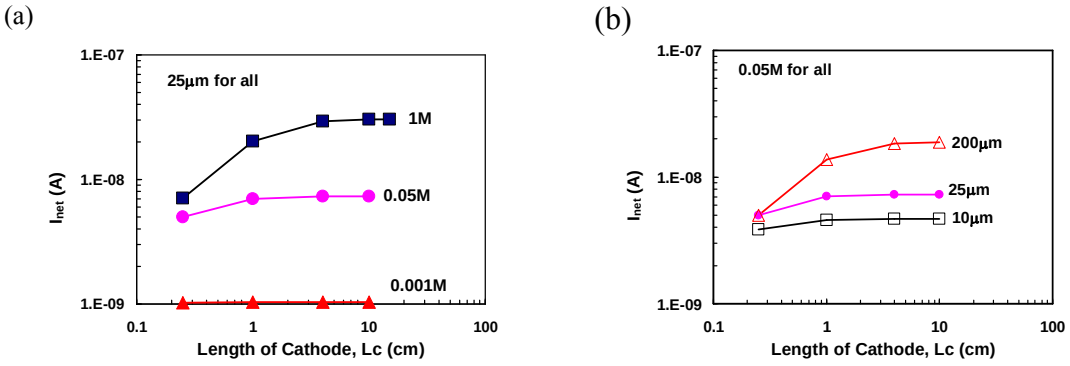

Figure 6. Interaction between parameters: (a) effect of Lc varies with $[Cl^-]$; (b) Effect of Lc varies with WL. I_{net} gradually saturated as Lc increased, and the speed of saturation depends on $[Cl^-]$ and on WL. (Extra calculations for selected cases with Lc=4 or 15 cm, were performed to reveal the saturation phenomenon.)

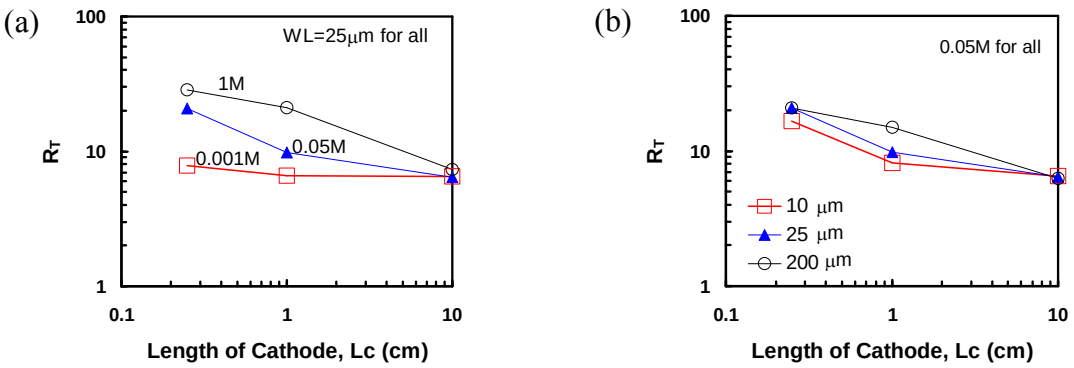

Figure 7. Effect of Temperature, as described by $R_T = I_{net}(T=95^oC)/I_{net}(T=25^oC)$. Regardless of $[Cl^-]$ or WL, R_T tends to asymptote to ~6.5 at large Lc.

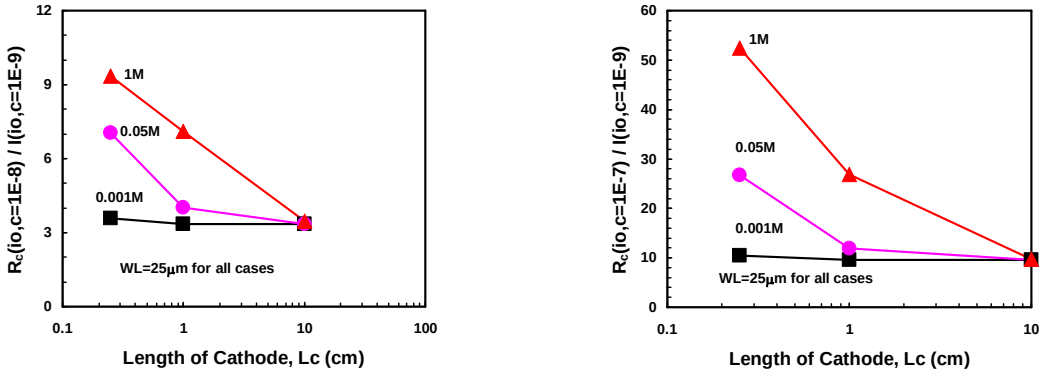

Figure 8. Effect of Cathodic exchange current density $i_{o,c}$. Regardless of $[Cl^-]$, Rc tends to stabilize with increasing Lc

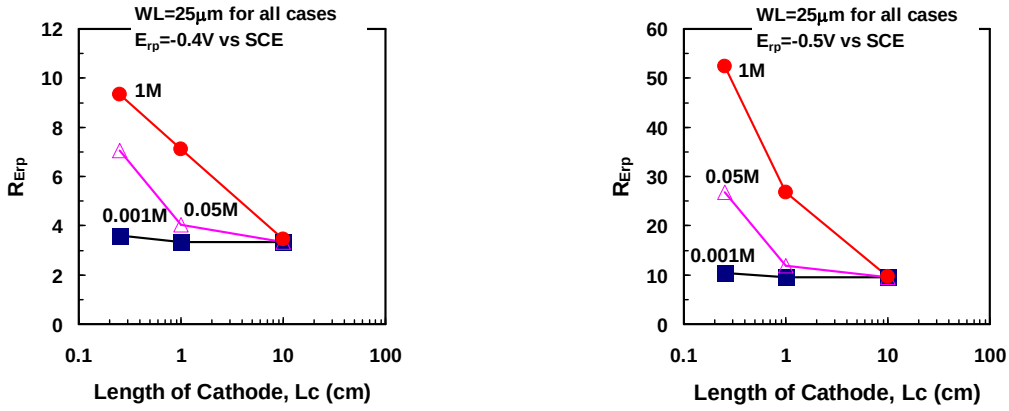

Figure 9. Effect of E_{rp}, $R_{Erp}=I_{net}(E_{rp}=-0.4 \text{ or } -0.5V)/ I_{net}(E_{rp}=-0.3V)$. Regardless of $[Cl^-]$, R_{Erp} tends to stabilize with increasing Lc

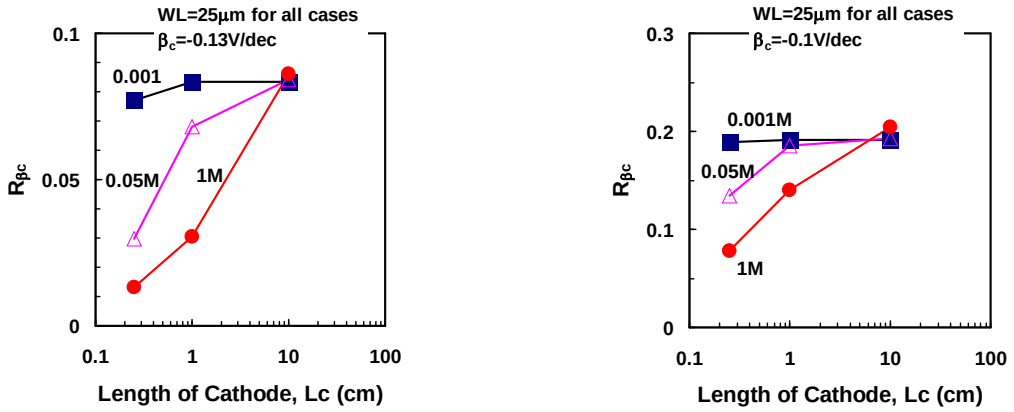

Figure 10. Effect of β_c, as described by $R_{\beta c}=I_{net}(\beta_c$ =0.13 or 0.1V)/$I_{net}(\beta_c$ =0.06V): a) βc=0.13 V/dec; b) βc=0.1 V/dec. Regardless of [Cl^-], R_c tends to asymptote to ~0.084 (βc=0.13 V/dec) and ~0.2 (βc=0.1 V/dec) respectively at large Lc.

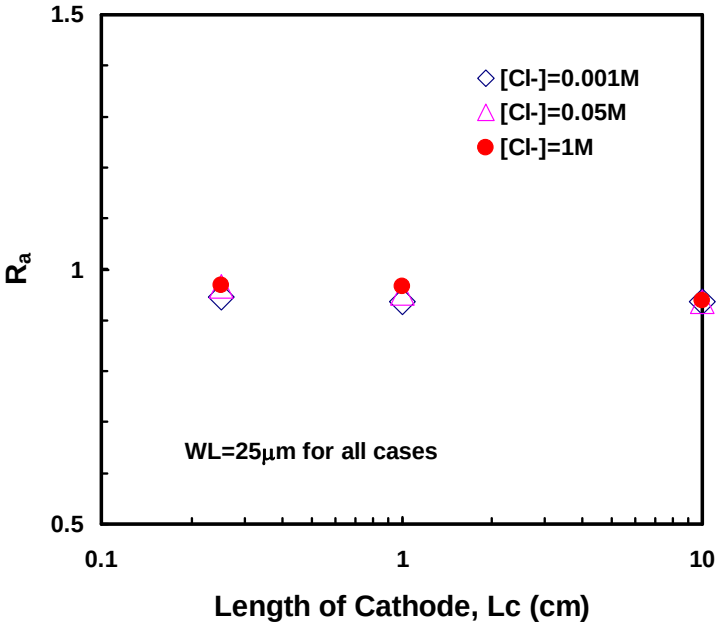

Figure 11. Effect of passive current density i_p, described by $R_a=I_{net}(i_p=10^{-6})/I_{net}(i_p=10^{-7})$. R_a was 0.9496±0.0015 for all cases regardless of values of Lc and [Cl^-].

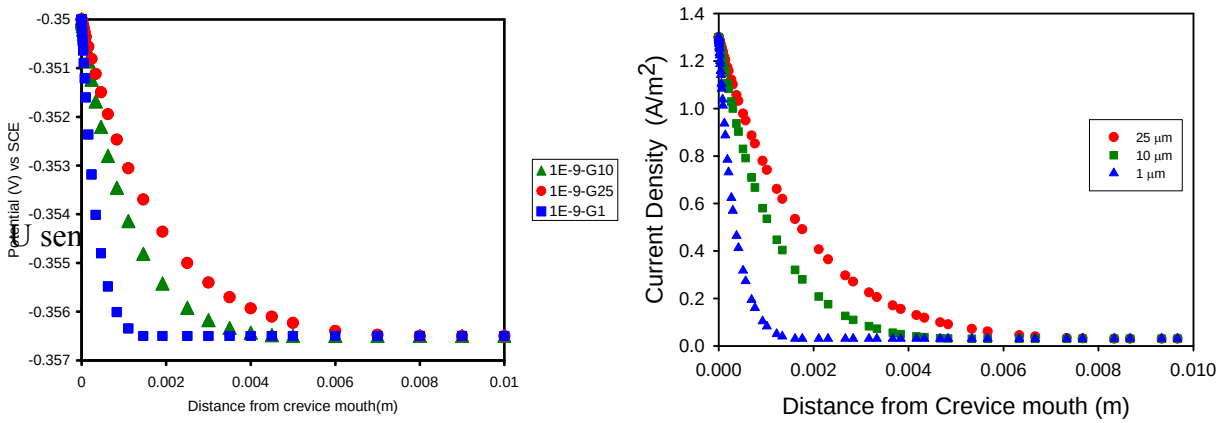

Figure 12. Typical potential and current output for crevice

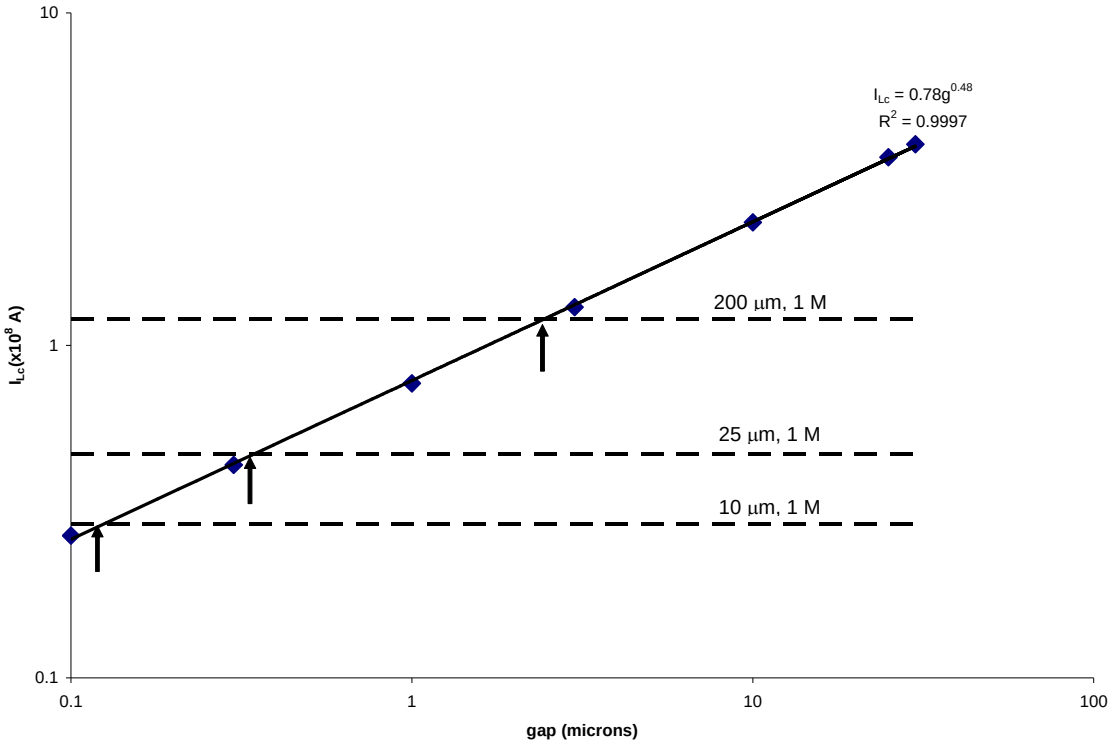

Figure 13. Stability of crevices linked to wetted external cathode. Total current demand of anode is related to the crevice gap via a power law with an exponent of 0.48. The dotted lines represent the maximum current from wetted external cathodes with different water layer thicknesses and a constant solution composition. Only crevices with gaps < 10 µm can be stabilized by such cathodes.